shifting atmosphere-ocean circulation patterns, with the tendency for global radiative surface warming being countered by the ocean dynamical thermostat.

References and Notes

1. J. L. Lean, *Geophys. Res. Lett.* **27**, 2425 (2000).
2. G. A. Meehl, J. M. Arblaster, K. Matthes, F. Sassi, H. van Loon, *Science* **325**, 1114 (2009).
3. M. E. Mann, M. A. Cane, S. E. Zebiak, A. Clement, *J. Clim.* **18**, 447 (2005).
4. A. C. Clement, R. Seager, M. A. Cane, S. E. Zebiak, *J. Clim.* **9**, 2190 (1996).
5. K. M. Cobb, C. D. Charles, H. Cheng, R. L. Edwards, *Nature* **424**, 271 (2003).
6. M. E. Mann *et al.*, *Science* **326**, 1256 (2009).
7. G. A. Vecchi, A. Clement, B. J. Soden, *Eos* **89**, 81 (2008).
8. A. van Geen *et al.*, *Paleoceanography* **18**, 1098 (2003).
9. R. W. Reynolds, N. A. Rayner, T. M. Smith, D. C. Stokes, W. Q. Wang, *J. Clim.* **15**, 1609 (2002).
10. F. B. Schwing, M. O'Farrell, J. M. Steger, K. Baltz, "Coastal Upwelling Indices West Coast of North America 1946-96," *NOAA Tech. Memo. NOAA-TM-NMFS-SWSFC-231* [National Oceanic and Atmospheric Administration (NOAA), Washington, DC, 1996].
11. F. B. Schwing, T. Murphree, L. deWitt, P. M. Green, *Prog. Oceanogr.* **54**, 459 (2002).
12. R. Durazo, T. R. Baumgartner, *Prog. Oceanogr.* **54**, 7 (2002).
13. Methods are available as supporting material on *Science* Online.
14. L. R. Sautter, R. C. Thunell, *Paleoceanography* **6**, 307 (1991).
15. L. Stott *et al.*, *Nature* **431**, 56 (2004).
16. A. Koutavas, P. B. deMenocal, G. C. Olive, J. Lynch-Stieglitz, *Geology* **34**, 993 (2006).
17. J. A. Barron, D. Bukry, *Palaeogeogr. Palaeoclimatol. Palaeoecol.* **248**, 313 (2007).
18. T. D. Herbert *et al.*, *Science* **293**, 71 (2001); 10.1126/science.1059209.
19. A. Koutavas, J. P. Sachs, *Paleoceanography* **23**, PA4205 (2008).
20. G. Leduc, R. Schneider, J. H. Kim, G. Lohmann, *Quat. Sci. Rev.* **29**, 989 (2010).
21. A. C. Clement, R. Seager, M. A. Cane, *Paleoceanography* **15**, 731 (2000).
22. B. L. Otto-Bliesner, E. C. Brady, S.-I. Shin, Z. Liu, C. Shields, *Geophys. Res. Lett.* **30**, 2198 (2003).
23. A. B. G. Bush, *Geophys. Res. Lett.* **26**, 99 (1999).
24. Z. Liu, J. Kutzbach, L. Wu, *Geophys. Res. Lett.* **27**, 2265 (2000).
25. C. Morrill, J. T. Overpeck, J. E. Cole, *Holocene* **13**, 465 (2003).
26. P. J. Reimer *et al.*, *Radiocarbon* **46**, 1029 (2004).
27. R. C. Finkel, K. Nishiizumi, *J. Geophys. Res. Oceans* **102**, 26699 (1997).
28. M. Vonmoos, J. Beer, R. Muscheler, *J. Geophys. Res. Space Phys.* **111**, A10105 (2006).
29. J. Emile-Geay, M. Cane, R. Seager, A. Kaplan, P. Almasi, *Paleoceanography* **22**, PA3210 (2007).
30. P. J. Webster *et al.*, *J. Geophys. Res.* **103**, 14451 (1998).
31. Y. J. Wang *et al.*, *Science* **308**, 854 (2005).
32. U. Neff *et al.*, *Nature* **411**, 290 (2001).
33. R. B. Alley *et al.*, *Geology* **25**, 483 (1997).
34. G. Bond *et al.*, *Science* **294**, 2130 (2001); 10.1126/science.1065680.
35. E. R. Cook, R. Seager, M. A. Cane, D. W. Stahle, *Earth Sci. Rev.* **81**, 93 (2007).
36. Y. Asmerom, V. Polyak, S. Burns, J. Rassmussen, *Geology* **35**, 1 (2007).
37. We thank P. Cappa, D. Lopez, D. Weller, and C. Wolak for laboratory assistance. This manuscript was improved by comments from B. Fox-Kemper and S. Lehman. This work was supported by collaborative NSF grants OCE-0214221 and OCE-0214646. R.M. is supported by the Royal Swedish Academy of Sciences through a grant financed by the Knut and Alice Wallenberg Foundation. Data are available at the NOAA National Climatic Data Center for Paleoclimatology.

Plasticity of Animal Genome Architecture Unmasked by Rapid Evolution of a Pelagic Tunicate

France Denoeud,[1,2,3] Simon Henriet,[4]* Sutada Mungpakdee,[4]* Jean-Marc Aury,[1,2,3]* Corinne Da Silva,[1,2,3]* Henner Brinkmann,[5] Jana Mikhaleva,[4] Lisbeth Charlotte Olsen,[4] Claire Jubin,[1,2,3] Cristian Cañestro,[6,24] Jean-Marie Bouquet,[4] Gemma Danks,[4,7] Julie Poulain,[1,2,3] Coen Campsteijn,[4] Marcin Adamski,[4] Ismael Cross,[8] Fekadu Yadetie,[4] Matthieu Muffato,[9] Alexandra Louis,[9] Stephen Butcher,[10] Georgia Tsagkogeorga,[11] Anke Konrad,[22] Sarabdeep Singh,[12] Marit Flo Jensen,[4] Evelyne Huynh Cong,[4] Helen Eikeseth-Otteraa,[4] Benjamin Noel,[1,2,3] Véronique Anthouard,[1,2,3] Betina M. Porcel,[1,2,3] Rym Kachouri-Lafond,[13] Atsuo Nishino,[14] Matteo Ugolini,[4] Pascal Chourrout,[15] Hiroki Nishida,[14] Rein Aasland,[16] Snehalata Huzurbazar,[12] Eric Westhof,[13] Frédéric Delsuc,[11] Hans Lehrach,[17] Richard Reinhardt,[17] Jean Weissenbach,[1,2,3] Scott W. Roy,[18] François Artiguenave,[1,2,3] John H. Postlethwait,[6] J. Robert Manak,[10] Eric M. Thompson,[4,19] Olivier Jaillon,[1,2,3] Louis Du Pasquier,[20] Pierre Boudinot,[21] David A. Liberles,[22] Jean-Nicolas Volff,[23] Hervé Philippe,[5] Boris Lenhard,[4,7,19] Hugues Roest Crollius,[9] Patrick Wincker,[1,2,3]† Daniel Chourrout[4]†

Genomes of animals as different as sponges and humans show conservation of global architecture. Here we show that multiple genomic features including transposon diversity, developmental gene repertoire, physical gene order, and intron-exon organization are shattered in the tunicate *Oikopleura*, belonging to the sister group of vertebrates and retaining chordate morphology. Ancestral architecture of animal genomes can be deeply modified and may therefore be largely nonadaptive. This rapidly evolving animal lineage thus offers unique perspectives on the level of genome plasticity. It also illuminates issues as fundamental as the mechanisms of intron gain.

Tunicates, viewed as the closest living relatives of vertebrates, were probably simplified from more complex chordate ancestors (*1*). Larvacean tunicates represent the second most abundant component of marine zooplankton and filter small particles by their gelatinous house. *Oikopleura dioica* is the most cosmopolitan larvacean, has a very short life cycle (4 days at 20°C), and can be reared in the laboratory for hundreds of generations (*2*). Unique among tunicates, it has separate sexes. We sequenced its genome with high-coverage shotgun reads (14X) using males resulting from 11 successive full-sib matings (figs. S1 and S2 and tables S1 to S3) (*3*). Two distinct haplotypes were retained, despite inbreeding. Their comparison yielded a high estimate of population mutation rate ($\theta = 4N_e\mu = 0.0220$) that is consistent with a large effective population size (N_e) and/or a high mutation rate per generation (μ) (*3*). Sequence comparisons among populations from the eastern Pacific and eastern Atlantic and within the latter revealed low dN/dS values (dN, rate of substitutions at nonsilent sites; dS, rate of substitutions at silent sites) consistent with strong purifying selection, as expected for large populations (*3*). In 17 of 18

[1]Commissariat à l'Énergie Atomique, Institut de Génomique, Genoscope, Evry, France. [2]CNRS, UMR 8030, Evry, France. [3]Université d'Evry, Evry, France. [4]Sars International Centre for Marine Molecular Biology, University of Bergen, Bergen, Norway. [5]Département de Biochimie, Université de Montréal, Montréal, Canada. [6]Institute of Neuroscience, University of Oregon, Eugene, OR 97403, USA. [7]Bergen Center for Computational Science, University of Bergen, Bergen, Norway. [8]Laboratorio de Genética, Universidad de Cádiz, Cádiz, Spain. [9]Dyogen Lab, Institut de Biologie de l'ENS (IBENS), CNRS-UMR8197, Ecole Normale Supérieure, Paris, France. [10]Department of Biology, University of Iowa, Iowa City, IA 52242–1324, USA. [11]Laboratoire de Paléontologie, Phylogénie et Paléobiologie, Institut des Sciences de l'Evolution, UMR 5554–CNRS, Université Montpellier II, Montpellier, France. [12]Department of Statistics, University of Wyoming, Laramie, WY 82071, USA. [13]Institut de Biologie Cellulaire et Moléculaire du CNRS, Université de Strasbourg, Strasbourg, France. [14]Department of Biological Sciences, Osaka University, Osaka, Japan. [15]Centre Hospitalier d'Albi, Albi, France. [16]Department of Molecular Biology, University of Bergen, Bergen, Norway. [17]Vertebrate Genomics, Max Planck Institute for Molecular Genetics, Berlin, Germany. [18]National Center for Biotechnology Information, National Library of Medicine, National Institutes of Health, Bethesda, MD 20894, USA. [19]Department of Biology, University of Bergen, Bergen, Norway. [20]Institute of Zoology and Evolutionary Biology, University of Basel, Basel, Switzerland. [21]Institut National de la Recherche Agronomique (INRA), Virologie et Immunologie Moléculaires, Jouy-en-Josas, France. [22]Department of Molecular Biology, University of Wyoming, Laramie, WY 82071, USA. [23]Institut de Génomique Fonctionnelle de Lyon, UMR 5242–CNRS/INRA/Université Claude Bernard Lyon 1/Ecole Normale Supérieure, Ecole Normale Supérieure de Lyon, Lyon, France. [24]Departament de Genètica, Universitat de Barcelona, Spain.

*These authors contributed equally to this work.
†To whom correspondence should be addressed. E-mail: Daniel.Chourrout@sars.uib.no (D.C.); pwincker@genoscope.cns.fr (P.W.)

phylogenetic trees constructed with 26 metazoan genomes and nine independent data sets, *Oikopleura* shows the fastest protein evolution, and even higher evolutionary rates are observed for mitochondrial genes that are heavily modified by oligo-dT insertions (figs. S3 to S6 and tables S4 to S6) (*3*). Key components of DNA repair, especially in the nonhomologous end-joining pathway, were not detected in the genome (fig. S7 and table S7) (*3*). Coincident rapid evolution of nuclear and mitochondrial genomes may also reflect a highly mutagenic context at the ocean surface.

At 70 megabases with 18,020 predicted genes, the *Oikopleura* genome is unusually compact. Introns are very small (peak at 47 base pairs, 2.4% > 1 kb), as are intergenic spaces, partly because of numerous operons (fig. S8 and table S8) (*3*). Genes outside operons are also densely packed (53% of intergenic distances < 1 kb). Even compared with other compact genomes (*4*), the density of transposable elements (TEs) is low. Most pan-animal TE superfamilies are absent in *Oikopleura*, and only two species-specific clades of retrotransposons (*5*) have diversified. A massive purge of ancient TEs can be invoked, but TEs currently present in the genome show multiple signs of activity (figs. S9 to S16) (*3*). The low copy number of each element and the uneven genome distribution of the main TE clades suggest tight control of their proliferation (Fig. 1A) (*3*).

Two exceptions to global compaction are particularly interesting, as they may illustrate where excessive reduction is harmful. First, a small population of *Oikopleura* genes has relatively large introns and intergenic spaces (Fig. 1B). It is enriched for developmentally regulated transcription

Table 1. Minimal immune system predicted from the *Oikopleura* genome. Numbers of genes or domains in families encoding potential immunity factors. *D.m.*, *Drosophila melanogaster*; *S.p.*, *Strongylocentrotus purpuratus*; *O.d.*, *Oikopleura dioica*; *C.i.*, *Ciona intestinalis*; *B.f.*, *Branchiostoma floridae*; *P.m.*, *Petromyzon marinus*; *H.s.*, *Homo sapiens*. TLR, Toll-like receptor; NLR, NOD-like receptor; SRCR, scavenger receptor cysteine-rich; PGRP, peptidoglycan recognition protein; RIG-I, retinoic acid–inducible gene–I; IgSF-ITIM, immunoglobulin superfamily domain with immunoreceptor tyrosine inhibitory motif; DEATH-TIR, DEATH superfamily members with Toll/interleukin-1–receptor domain; SARM1, SAM- and ARM-containing protein 1; TIRAP, Toll/interleukin-1–receptor domain-containing adapter protein; TICAM2, Toll/interleukin-1–receptor domain-containing adapter molecule; PLA2, phospholipase A2. ND, not determined.

	D.m.	S.p.	O.d.	C.i.	B.f.	P.m.	H.s.
Sensors							
TLR	9	222	1	3	48	21	10
NLR	0	203	0	20	92	140–220	20
SRCR	14	218	1	81	270	287	81
PGRP	15	5	4	6	>20	ND	6
RIG-I–like helicases	0	12	0	ND	7	ND	3
C-type lectins	32	104	31	120	1215	ND	81
IgSF-ITIM	>3	ND	5	>6	>5	>3	>50
Adaptors							
MyD88-like (DEATH-TIR)	1	4	0	1	4	ND	1
SARM1-like, TIRAP-like, TICAM2-like	1	15	0	>2	12	ND	3
Potential effector							
PLA2	8	65	128	7	>7	ND	11

Fig. 1. Genome compaction features. (**A**) Chromosome regions assembled with physical links and genetic markers. The location of TEs is indicated with horizontal lines (lines on the left sides, DNA transposons; lines on right sides, short lines for long terminal repeat–retrotransposons and long lines for long interspersed elements). (**B**) Distribution of gene models over 10% abundance classes of intron size and upstream intergenic distance for 8812 nonoperon genes (left) and for 189 developmentally regulated genes, mainly transcription factors (right). (**C**) Conserved elements revealed in genome alignments of Atlantic and Pacific ocean populations of *O. dioica*: density of conserved blocks (top), gene annotation (middle), and perfectly conserved elements >100 bp (bottom gray line) (blue, Norway versus northwest America; red, Norway versus Japan). (**D**) Giant Y genes and their testis expression revealed by reverse transcription polymerase chain reaction and in situ hybridization. hpf, hours post fertilization; ctrl, control. The arrowhead indicates the giant gene expression product.
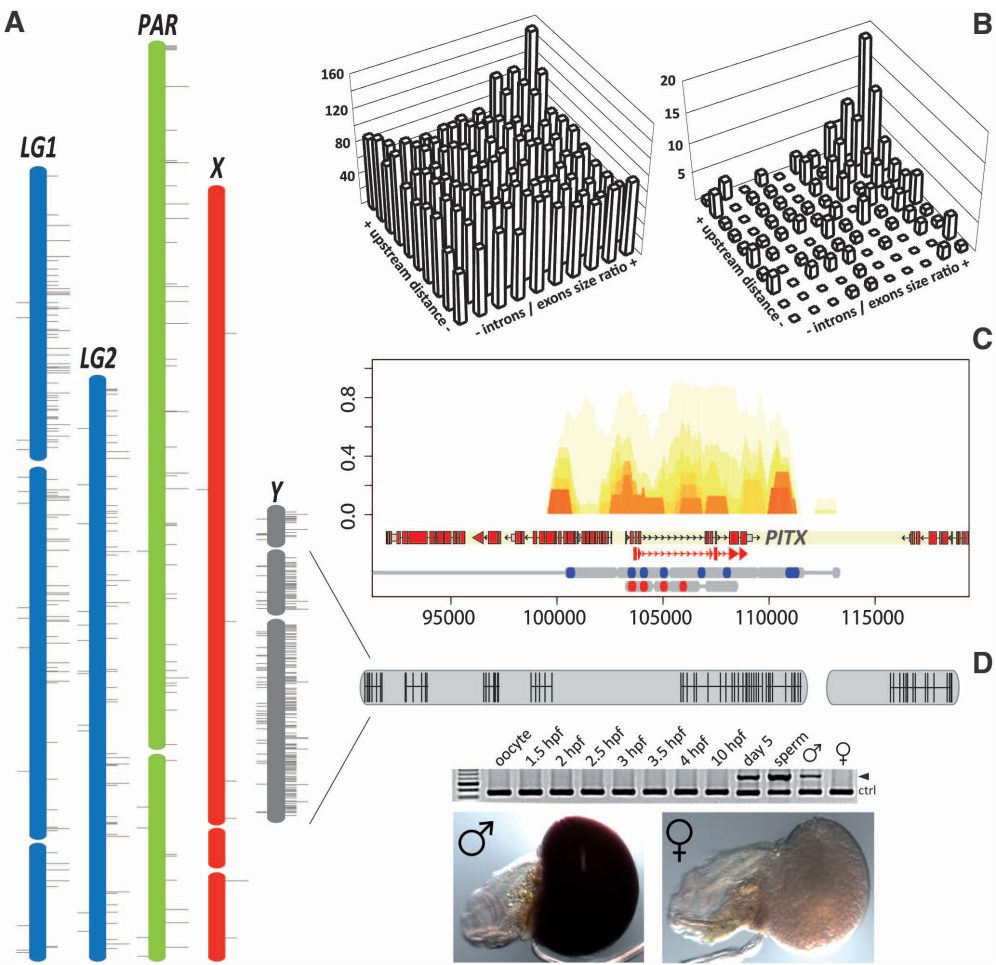
factor genes that are long in other genomes because of an abundance of regulatory elements (6). Regulatory-element sequences can be highly conserved, though rarely across phyla, and *Oikopleura* homologs of vertebrate conserved elements were not detected (3). However, a comparison of genes encoding developmental transcription factors from Atlantic and Pacific *O. dioica* revealed short segments of higher sequence conservation in noncoding regions than in exons, suggestive of a rich regulatory content (Fig. 1C and fig. S17) (3). Interestingly, in a revolution of massive intron loss (see below), *Oikopleura* retained large introns more often than small ones, and the ratio of ancestral to newly acquired introns is highest in developmental transcription factor genes (figs. S18 and S19) (3).

Second, Mendelian analysis showed that sex in *Oikopleura* is genetically determined (fig. S20 and table S10) (3), and we could reconstruct large X and Y chromosomes (Fig. 1A). Seven genes on the Y chromosome, all expressed in the testis during spermatogenesis, have giant introns (Fig. 1D). Their size probably grew with the nonrecombining Y chromosome region, flaunting global compaction.

Fig. 2. Introns and intron gain scenarios. (**A**) Main intron logos. (**B**) Transposon insertion: Duplicated insertion sites (framed in blue) allow miniature inverted repeat transposable element (MITE)–like insertions to be spliced out exactly (red, exons; black, introns). (**C**) Reverse splicing: four pairs of homologous introns (black) and their immediate exonic environments (red).
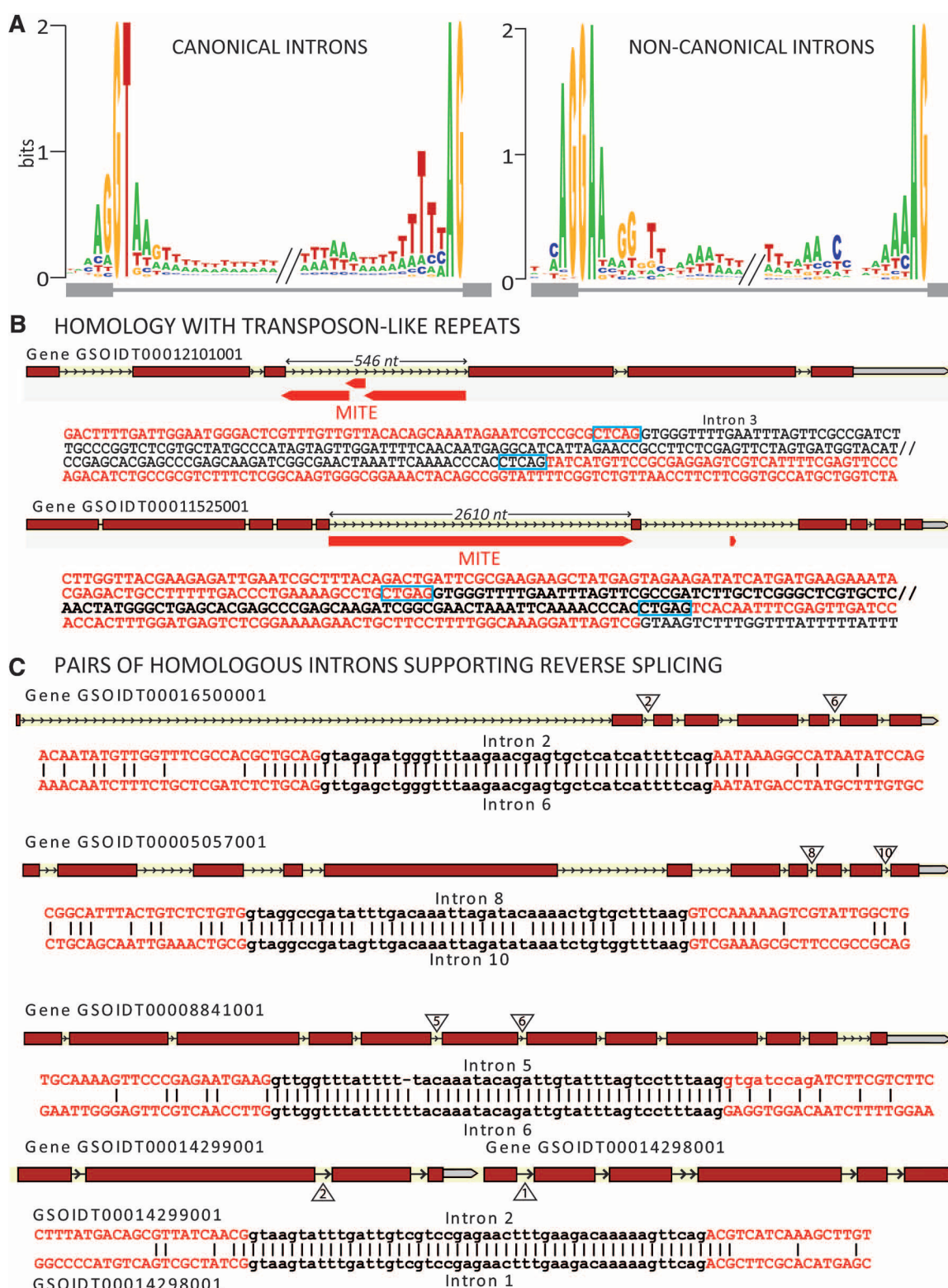
Oikopleura has a rather common number of introns per gene (4.1), but the turnover of its introns has been extraordinarily high: Of 5589 introns mapped by interspecies protein alignments, 76% had positions unique to *Oikopleura* (newly acquired introns), 17% were at ancestral positions (old introns), and 7% could not be classified (fig. S21) (*3*). Non-canonical introns, mostly GA-AG and with a very specific acceptor site, are unusually frequent (12%) (Fig. 2A and figs. S22 to S25) (*3*). They show several peculiarities (tables S11 and S12), including preferential insertion in phase 1, which is compatible with the current codon usage, as would be expected for the most recently gained introns (*3*, *7*). The most distinctive feature of newly acquired introns (figs. S26 and S27 and tables S13 to S15) is that they are more often noncanonical than old introns (8.4 versus 2.6%) (*3*). Because *Oikopleura* lacks the minor spliceosome and has only one type of each spliceosomal component, we propose that a single and permissive major spliceosome is used, with U1snRNP (where snRNP is small nuclear ribonucleoprotein) and U2AF able to recognize donor and acceptor sites (*3*, *8*, *9*). cDNA sequence information suggests an efficient splicing for the vast majority of introns. A permissive spliceosome could favor intron gains by correctly splicing out newly acquired introns. The pattern

of intron loss in *Oikopleura* is consistent with homologous recombination of reverse transcribed mRNA (table S16) (*3*, *10*). Among hypothetical mechanisms of intron gain, we provide evidence for the insertion of transposon-like elements and, more remarkably for reverse splicing, a reaction in which spliced out introns can be ectopically reinserted into transcripts (*11*). We identified 32 compelling candidate introns for transposon insertion (Fig. 2B and table S17) (*3*), those matching repetitive elements containing terminal repeats at almost all nucleotides, with exons excluded. These introns were usually hemizygous in genotyped individuals, but one individual was homozygous and displayed spliced transcripts (figs. S28 to S30 and table S18) (*3*). We also identified four pairs of nearly identical introns (NIIs) with no or very weak similarity in flanking exons (Fig. 2C) (*3*), which, to the best of our knowledge, represent the first reported candidates for reverse splicing (*12*). All animals were homozygous for NIIs and had spliced transcripts (fig. S31 and table S19) (*3*). Notably, introns of each pair of NIIs were found within the same gene or the same operon, suggesting intron propagation within their pre-mRNA. Many newly acquired introns of *Oikopleura* might have been propagated like these four NIIs before their sequences diverged, because they tend to be adjacent

in their host gene (table S20) (*3*). Competing mechanisms remain possible: First, introns could be reverse spliced into the genome itself, as can group II introns (*13*). Some, and possibly many, introns of *Oikopleura* could originate by repair of double strand breaks (DSBs), as proposed for newly acquired introns in *Daphnia* (*14*). However, for the four mentioned intron pairs, a repair after a DSB would not readily explain the systematic colocalization of homologous introns in the same transcription unit. No feature in the sequences of those introns in pairs and their surroundings brings particular support for this mechanism (*3*).

We explored the *Oikopleura* genome for genes involved in either development or immunity. Many conserved immunity genes failed detection, supporting a minimized immune system consistent with the short *Oikopleura* life history (Table 1 and table S21) (*3*). Although frequent gene losses may have affected families of developmental genes, we were most intrigued by an unusually large number of lineage-specific duplicates, thus far reported for homeobox genes only (*15*): 87 amplifications accounting for 266 current genes (table S22) (*3*), versus 40 amplifications in *Ciona* giving 106 current genes (*16*). A survival analysis of early duplicates in the genome showed that duplicates are initially lost very rapidly with less relaxed selec-

Fig. 3. Gene duplications and loss of ancestral syntenies. (**A**) Early gene duplicates. (Main panel) Histogram of binned recent duplicate pairs; a mixture model (discrete distribution plus truncated Weibull distributions) accommodating heterogeneous birth/death processes is fitted. (Inset) Nonsynonymous substitution accumulation declines with ongoing synonymous substitution. (**B**) Expression of amplified homeobox gene groups in the trunk epithelium of larvae (red arrowheads). hD, hours dorsal view; hL, hours lateral view; hDL, hours dorsolateral view. (**C**) Loss of ancestral gene order. Positions of orthologous genes in a given metazoan genome (*y* axis) compared with ancestral chordate linkage groups [(CLGs), *x* axis]. The width of CLGs corresponds to the number of orthologs in a given species. Amphioxus and sea anemone genome segments represent the largest 25 assembled scaffolds, whereas *Ciona*, nematode, and *Oikopleura* segments are chromosomes.
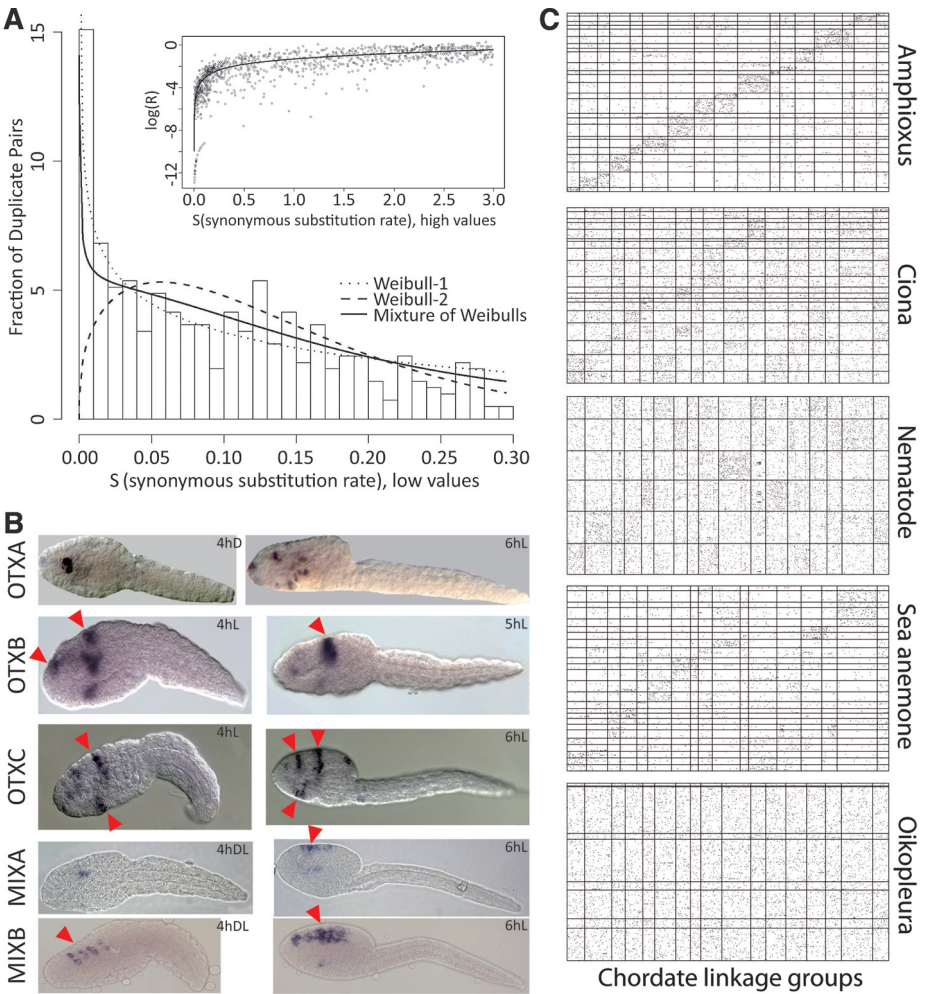
tion than in mammalian genomes (*17*). In contrast, those that survive beyond 0.02 dS units are relatively more likely to be retained (Fig. 3A, figs. S32 to S34, and table S23) (*3*). To understand how older developmental gene duplicates are used, we focused on homeobox genes. Notably, we detected broad expression signals in the larval trunk epithelium for genes of most amplified groups (16 in 20), but rarely for other groups (1 in 19) (Fig. 3B, fig. S35, and table S24), likely reflecting roles in patterning of the house-building epithelium (*18*), a crucial novelty of larvaceans. A preferential retention of duplicates for developmental genes has occurred in vertebrates after whole-genome duplications. Their massive retention in *Oikopleura* is exceptional among invertebrates. In addition to neofunctionalization for complex innovations like house production, another explanation may take into consideration the general reduction of gene size in *Oikopleura*. This may enhance the likelihood for developmental genes to escape truncation after the local rearrangements that cause duplications (*19*). Other mechanisms may facilitate duplications or preserve developmental gene duplicates in *Oikopleura*.

Finally, we compared synteny relationships in *Oikopleura* and several invertebrates to ancestral chordate linkage groups (*3*, *20*). Amphioxus, *Ciona*, *Caenorhabditis*, and sea anemone showed many cases of conserved chromosomal synteny (Fig. 3C, figs. S36 and S37, and table S25), but *Oikopleura* orthologs showed no such conservation. We also measured local synteny conservation between the same species and human (*3*). Amphioxus, *Ciona*, *Caenorhabditis*, and sea anemone (to a much lower degree) displayed significantly higher conservation of neighborhood than expected by chance. *Oiko-*

pleura showed a local gene order that is indistinguishable from random for distances smaller than 30 genes and a modest level of conserved synteny at larger distances (fig. S38).

We show that multiple genome-organization features, conserved across metazoans including other tunicates and nonbilaterians, have dramatically changed in the *Oikopleura* lineage. Despite an unprecedented genome revolution, the *Oikopleura* lineage preserved essential morphological features, even maintaining the chordate body plan to the adult stage, unlike other tunicates. Evolution in this lineage was rapid and probably took place in a context favoring purifying selection against mildly deleterious features. Our results strengthen the view that global similarities of genome architecture from sponges to humans (*20*–*23*) are not essential for the preservation of ancestral morphologies, as is widely believed (*24*–*26*).

References and Notes

1. F. Delsuc, H. Brinkmann, D. Chourrout, H. Philippe, *Nature* **439**, 965 (2006).
2. J. M. Bouquet *et al.*, *J. Plankton Res.* **31**, 359 (2009).
3. Supporting methods and results are available on *Science* Online.
4. T. H. Eickbush, A. V. Furano, *Curr. Opin. Genet. Dev.* **12**, 669 (2002).
5. J. N. Volff, H. Lehrach, R. Reinhardt, D. Chourrout, *Mol. Biol. Evol.* **21**, 2022 (2004).
6. A. Woolfe *et al.*, *PLoS Biol.* **3**, e7 (2005).
7. H. D. Nguyen, M. Yoshihama, N. Kenmochi, *BMC Evol. Biol.* **6**, 69 (2006).
8. M. Marz, T. Kirsten, P. F. Stadler, *J. Mol. Evol.* **67**, 594 (2008).
9. D. A. R. Zorio, T. Blumenthal, *Nature* **402**, 835 (1999).
10. T. Mourier, D. C. Jeffares, *Science* **300**, 1393 (2003).
11. S. W. Roy, W. Gilbert, *Nat. Rev. Genet.* **7**, 211 (2006).
12. S. W. Roy, M. Irimia, *Trends Genet.* **25**, 67 (2009).
13. B. Cousineau *et al.*, *Cell* **94**, 451 (1998).
14. W. Li, A. E. Tucker, W. Sung, W. K. Thomas, M. Lynch, *Science* **326**, 1260 (2009).
15. R. B. Edvardsen *et al.*, *Curr. Biol.* **15**, R12 (2005).
16. Y. Satou, N. Satoh, *Dev. Genes Evol.* **213**, 211 (2003).
17. T. Hughes, D. A. Liberles, *J. Mol. Evol.* **65**, 574 (2007).
18. E. M. Thompson, T. Kallesøe, F. Spada, *Dev. Biol.* **238**, 260 (2001).
19. V. Katju, M. Lynch, *Genetics* **165**, 1793 (2003).
20. N. H. Putnam *et al.*, *Nature* **453**, 1064 (2008).
21. N. H. Putnam *et al.*, *Science* **317**, 86 (2007).
22. M. Srivastava *et al.*, *Nature* **466**, 720 (2010).
23. M. Srivastava *et al.*, *Nature* **454**, 955 (2008).
24. M. Lynch, J. S. Conery, *Science* **302**, 1401 (2003).
25. M. Lynch, *Mol. Biol. Evol.* **23**, 450 (2006).
26. M. Lynch, *Proc. Natl. Acad. Sci. U.S.A.* **104** (suppl. 1), 8597 (2007).
27. The Sars Centre budget, the Functional Genomics (FUGE) Programme of the Norwegian Research Council, Genoscope, and NSF grants IOS-0719577 and DBI-0743374 supported the research. This is publication ISEM-2010-123 of the Institut des Sciences de l'Evolution de Montpellier. GENBANK/European Molecular Biology Laboratory sequence accession numbers are CABV01000001-CABV01005917, CABW01000001-CABW01006678, FN653015-FN654274, FN654275-FN658470, FP700189-FP710243, FP710258-FP791398, and FP791400-FP884219. The sequence data for *Capitella teleta*, *Daphnia pulex*, *Helobdella robusta* and *Lottia gigantea* were produced by the U.S. Department of Energy Joint Genome Institute (www.jgi.doe.gov/) in collaboration with the community of users. We thank I. Ahel, B. Haubold, and one anonymous reviewer for generous advice. This article is dedicated to Hans Prydz and Kåre Rommetveit for their pioneer roles in the Sars Centre establishment.

Rewiring of Genetic Networks in Response to DNA Damage

Sourav Bandyopadhyay,[1] Monika Mehta,[2] Dwight Kuo,[3] Min-Kyung Sung,[4] Ryan Chuang,[3] Eric J. Jaehnig,[5] Bernd Bodenmiller,[6] Katherine Licon,[1] Wilbert Copeland,[3] Michael Shales,[7] Dorothea Fiedler,[7,8] Janusz Dutkowski,[1] Aude Guénolé,[9] Haico van Attikum,[9] Kevan M. Shokat,[7,8] Richard D. Kolodner,[5,1,10] Won-Ki Huh,[4] Ruedi Aebersold,[6] Michael-Christopher Keogh,[2]* Nevan J. Krogan,[7]* Trey Ideker[1,3,10]*

Although cellular behaviors are dynamic, the networks that govern these behaviors have been mapped primarily as static snapshots. Using an approach called differential epistasis mapping, we have discovered widespread changes in genetic interaction among yeast kinases, phosphatases, and transcription factors as the cell responds to DNA damage. Differential interactions uncover many gene functions that go undetected in static conditions. They are very effective at identifying DNA repair pathways, highlighting new damage-dependent roles for the Slt2 kinase, Pph3 phosphatase, and histone variant Htz1. The data also reveal that protein complexes are generally stable in response to perturbation, but the functional relations between these complexes are substantially reorganized. Differential networks chart a new type of genetic landscape that is invaluable for mapping cellular responses to stimuli.

One of the most basic approaches to understanding gene function relies on the identification of genetic interactions, which occur when the phenotypic effects of one gene depend on the presence of a second. Recently, a number of technologies have been developed to systematically map genetic interaction networks over large sets of genes in budding yeast (*1*–*3*) and other model organisms (*4*, *5*). Thus far, these networks have been constructed only under normal laboratory conditions. However, cells are constantly bombarded by signals and stresses, such as ligands, drugs, hormones, toxins, or other

[1]Department of Medicine, University of California, San Diego, La Jolla, CA 92093, USA. [2]Department of Cell Biology, Albert Einstein College of Medicine, Bronx, NY 10461, USA. [3]Department of Bioengineering, University of California, San Diego, La Jolla, CA 92093, USA. [4]School of Biological Sciences and Research Center for Functional Cellulomics, Institute of Microbiology, Seoul National University, 151-742 Seoul, Republic of Korea. [5]Ludwig Institute for Cancer Research and Department of Cellular and Molecular Medicine, University of California, San Diego, La Jolla, CA 92093, USA. [6]Institute of Molecular Systems Biology, ETH Zürich, Zürich CH 8093, Switzerland, and Faculty of Science, University of Zürich, Zürich CH 8057, Switzerland. [7]Department of Cellular and Molecular Pharmacology, University of California, San Francisco, San Francisco, CA 94158, USA. [8]Howard Hughes Medical Institute, San Francisco, CA 94158, USA. [9]Department of Toxicogenetics, Leiden University Medical Center, Leiden, Netherlands. [10]The Institute for Genomic Medicine, University of California, San Diego, La Jolla, CA 92093, USA.

*To whom correspondence should be addressed. E-mail: tideker@ucsd.edu (T.I.); krogan@cmp.ucsf.edu (N.J.K.); michael.keogh@einstein.yu.edu (M.-C.K.)